

On Extended Target Tracking Using PHD Filters

Karl Granström, Christian Lundquist, Fredrik Gustafsson
Division of Automatic Control
Department of Electrical Engineering
Linköping University, SE-581 83, Linköping, Sweden
Email: {karl,lundquist,fredrik}@isy.liu.se

Umut Orguner
Department of Electrical and Electronics Engineering
Middle East Technical University
06531, Ankara, Turkey
Email: umut@eee.metu.edu.tr

Abstract—This paper presents an overview of the extended target tracking research undertaken at the division of Automatic Control at Linköping University. The PHD and CPHD filters for multiple extended target tracking under clutter and unknown association are summarized, with focus on the Gaussian mixture and Gaussian inverse Wishart implementations. The paper elaborates on measurement set partitioning, the measurement generating Poisson rates, the probability of detection, and practical examples of measurement models.

Index Terms—Finite Set Statistics, Probability Hypothesis Density, Extended Targets, Gaussian, Wishart,

I. INTRODUCTION

In target tracking it is often assumed that a single target will give rise to at most one measurement per time step, see e.g. [1]–[3]. In many modern applications, the sensor and target setup is such that this assumption no longer holds. When a target occupies multiple sensor resolution cells, it can potentially give rise to more than one measurement per time step. Such a target is called *extended target*.

A typical situation where the sensor can give multiple detections for a single target occurs in urban traffic. Consider Figure 1, where a car, a cyclist and a pedestrian were detected by a laser range scanner. The car is L-shaped because only two sides are visible to the sensor, the cyclist looks like a stick with a dot in the middle and the two legs of the pedestrian are visible as paired dots. These are good examples of extended targets, because they have each caused multiple detections.

In the traffic situation in Figure 1, several targets are present, and the number of targets varies as the targets move relative to the sensor, and it is *a priori* unknown which target caused which measurement. This is an example of a typical multi target tracking problem, and there exists several frameworks in the literature to handle multiple targets under uncertain association and clutter. One approach is to model the targets as a *random finite set* (RFS), and try to estimate this set, i.e., both estimating the elements of the set and the number of elements in the set. Mahler [4], [5] has introduced an approach, called finite set statistics (FISST), which allows the problem of estimating multiple targets in clutter with uncertain associations to be cast in a Bayesian filtering framework. An important contribution of FISST is to provide structured tools for Bayesian estimation, in the form of the statistical moments

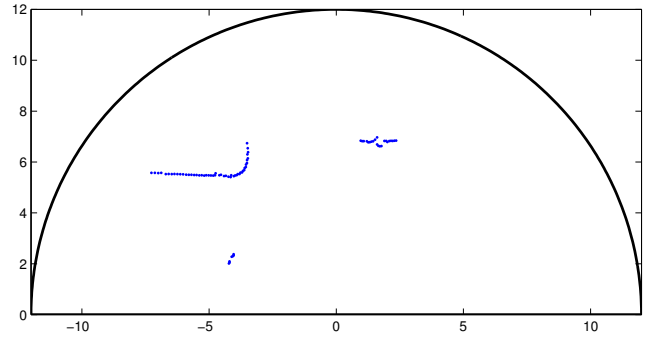


Fig. 1. Example of laser range data, featuring detections obtained from a car, a cyclist and a pedestrian.

of a RFS. The first order moment of a RFS is called *probability hypothesis density* (PHD), and is an intensity function defined over the state space of the targets. In all but the simplest of cases, the full multi-target Bayesian filter is infeasible to implement. As an approximation, the so called PHD filter propagates in time PHDs corresponding to the set of target states.

The standard PHD filter was developed to track targets which produces at most one measurement per time step. The topic of this paper is tracking of extended targets, such as those shown in Figure 1. Mahler [6] has presented an extension of the PHD filter to also handle extended targets, and the main purpose of this paper is to elaborate on different aspects of practical implementations of the extended target PHD filter.

The paper is organized as follows. In Section II we present the extended target PHD filter, and relate selected parts of its implementations to the scenario depicted in Figure 1. In Section III we give the extended target CPHD filter, and show that the CPHD filter has a more stable cardinality estimate than the PHD filter in situations where the probability of detection is (much) less than unity. The paper is ended with concluding remarks in Section IV.

II. THE EXTENDED TARGET PHD FILTER

In a Bayesian framework, the posterior is given by the product of the likelihood and the prediction. Let

$$D_{k|k-1}(\mathbf{x}|\mathbf{Z}) = D(\mathbf{x}_k|\mathbf{Z}^{k-1}) \quad (1)$$

be the predicted PHD, where \mathbf{x}_k is the multiple extended target state at time t_k , and \mathbf{Z}^{k-1} is the set of measurements up to, and including, time t_{k-1} . The posterior, or corrected, PHD $D_{k|k}(\mathbf{x}|\mathbf{Z})$, is given by

$$D_{k|k}(\mathbf{x}|\mathbf{Z}) = L_{\mathbf{Z}_k}(\mathbf{x}) D_{k|k-1}(\mathbf{x}|\mathbf{Z}), \quad (2)$$

where $L_{\mathbf{Z}_k}$ is the likelihood function. The likelihood function models the relation between the target states and the measurements. Further, it also models target states which might not give rise to measurements at all, as well as clutter measurements, which are measurements not generated by the targets.

In the specific case of extended targets, the likelihood function $L_{\mathbf{Z}_k}$ must also model the relationship between a single target state and the number of measurements that a single target might cause. Gilholm *et al* [7] presented a model for extended targets in which the number of measurements generated by an extended target is a random draw from a Poisson distribution. The so called PHD pseudo-likelihood function for the extended target Poisson model of [7] was derived in [6], and is defined as

$$L_{\mathbf{Z}_k}(\mathbf{x}) \triangleq \overbrace{1 - \left(1 - e^{-\gamma(\mathbf{x})}\right) p_D(\mathbf{x})}^{\text{Not detected targets}} + \underbrace{e^{-\gamma(\mathbf{x})} p_D(\mathbf{x}) \sum_{\mathbf{p} \subseteq \mathbf{Z}_k} \omega_{\mathbf{p}} \sum_{W \in \mathcal{P}} \frac{\gamma(\mathbf{x})^{|W|}}{d_W} \cdot \prod_{\mathbf{z}_k \in W} \frac{p(\mathbf{z}_k|\mathbf{x})}{\lambda_k c_k(\mathbf{z}_k)}}_{\text{Detected targets}}, \quad (3)$$

where the first part models the non-detected targets, and the second part models the detected targets and the clutter measurements.

The notation $\mathbf{p} \subseteq \mathbf{Z}_k$ means that \mathbf{p} is a partition of the measurement set \mathbf{Z}_k , i.e. a division of the measurements \mathbf{z} into non-empty cells W . The first summation in (3) is taken over all possible partitions \mathbf{p} of the measurement set \mathbf{Z}_k , and the second summation is taken over all cells W in the current partition \mathbf{p} . The product in (3) is taken over all measurements \mathbf{z}_k in one cell W . Further, the quantities $\omega_{\mathbf{p}}$ and d_W are non-negative coefficients defined for each partition \mathbf{p} and cell W respectively.

To obtain a computationally tractable extended target PHD filter, a few assumptions and approximations are necessary. The full details are given in [8]–[10]. In what follows, selected parts of the extended target PHD filter are elaborated on, namely:

- approximations of the full set of partitions, see Section II-A,
- the measurement rate $\gamma(\mathbf{x})$ that governs the Poisson rate with which target measurements are generated, see Section II-B,
- the probability of detection $p_D(\mathbf{x})$, see Section II-C,
- approximations of the PHD intensity using distribution mixtures, and the corresponding target measurement likelihood models $p(\mathbf{z}_k|\mathbf{x})$, see Section II-D.

The clutter is modeled as Poisson distributed in number, with rate λ_k , and spatial distribution $c_k(\mathbf{z}_k)$. We will not elaborate further on clutter in this paper.

A. Partitioning the Measurement Set

The number of ways that a set \mathbf{Z} containing n measurements can be partitioned is given by the n :th Bell number [11], denoted B_n . The Bell numbers B_n increase very fast when n increases, e.g. $B_3 = 5$, $B_5 = 52$ and $B_{10} = 115975$. In [6] Mahler points out that a tractable implementation of the extended target PHD filter requires approximations of the full set of partitions. The coefficients $\omega_{\mathbf{p}}$ in (3) can be interpreted as weights for the individual partitions \mathbf{p} , where a higher weight corresponds to a more likely partition. Any approximation of the full set of partitions should contain the most likely partitions.

Many sensors will produce sets of measurements where the subsets of measurements that stem from the same target are close with respect to some distance or measure. For radar and laser range sensors, the measurements will be close in terms of similar range and bearing. For imaging sensors, the measurements will be close e.g. in terms of pixel positions. Thus, in many scenarios a likely partition is one that places close measurements in the same cell, while keeping distant measurements in different cells.

Consider the measurements in Figure 1. From visual inspection of the measurements, one probable partition is given by the three cells in Figure 2a. This partition has clustered the measurements according to the belief that a person, a bicycle and a car were measured. An alternative partition, with four cells, is given in Figure 2b. Here one of the cells has been split in half, because what was believed to be measurements of a bicycle, could be measurements of two persons standing next to each other. Note that both partitions place measurements that are close in the same cell, yielding intuitive results.

The partitioning idea outlined above is used successfully in [8]–[10] to keep the number of partitions at a tractable level. For a set of thresholds, partitions are formed such that if the distance between two measurements is smaller than the threshold, they belong to the same cell, and otherwise to different cells. This partitioning algorithm, called Distance Partitioning [9], will always give a unique partition for a given threshold and a given set of measurements. The set of thresholds can be chosen in different ways, in [8]–[10] the Mahalanobis distance between two measurements is used to derive an upper and a lower limit for the thresholds used in Distance Partitioning.

A comparison between Distance Partitioning and K -means++, a well known clustering algorithm, shows that Distance Partitioning clearly outperforms K -means++, and that K -means++ only can match the performance of Distance Partitioning in scenarios with very low clutter rates [9]. Examples on how Distance Partitioning can be complemented with further partitioning methods are given in [9], [10].

When the full set of partitions is approximated with a subset, as outlined above, the tracking framework might seem

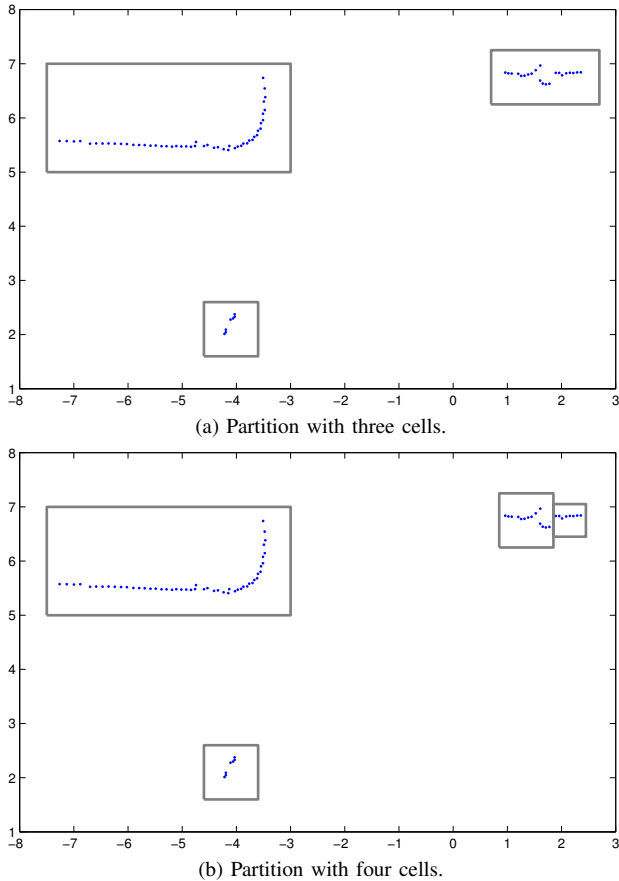


Fig. 2. Two possible partitions for the measurements in Figure 1, with three and four cells respectively. Note that there are many more possible partitions.

to be fragile to how the subset of partitions is computed. However, empirically we have found that this fragility only shows when too few partitions are included in the subset. When the subset of all partitions contains enough partitions, there is no performance degradation. Note also that in the implementations (see further in Section II-D), there is no explicit association between the PHD components and the partition cells – each PHD component is updated with each cell of each partition.

B. Measurement rate

The Poisson rate $\gamma(\mathbf{x})$ determines (the expected value of) how many measurements a target will produce in each time step. In [8]–[10] it is approximated as a non-negative function of the target state estimates, $\gamma(\mathbf{x}) \approx \gamma(\hat{\mathbf{x}})$ where $\hat{\mathbf{x}}$ is an estimate of \mathbf{x} .

When multiple targets are spatially close, they will give rise to close measurements, which are then typically partitioned into the same cells using Distance Partitioning. If the true value of $\gamma(\cdot)$ is known, this situation can be solved using additional partitioning methods, see [9], [10]. The sensitivity of the corresponding filter parameter, denoted $\hat{\gamma}(\cdot)$, is analyzed in [9]. Under the assumption that γ is constant over time and equal for all targets, a simulation study has shown that when the true parameter is within one standard deviation of the filter

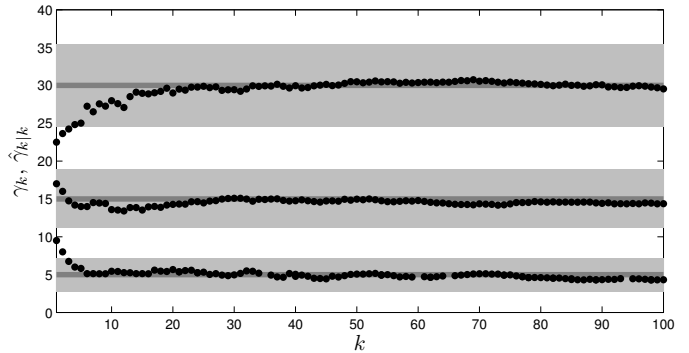


Fig. 3. Three targets with true rates $\gamma_k^{(1)} = 5$, $\gamma_k^{(2)} = 15$ and $\gamma_k^{(3)} = 30$, show as dark gray lines. The estimates $\hat{\gamma}_{k|k}^{(i)}$, shown as black dots, remain within the bounds $\gamma_k^{(i)} \pm \sqrt{\gamma_k^{(i)}}$, i.e. the true mean \pm one standard deviation, shown as light gray areas. Plot from [13].

parameter, the filter produces a correct cardinality estimate [9]. Note that when the extended targets are not close, the filter will give correct cardinality estimate even when γ is outside this range [9].

However, in the general case $\gamma(\cdot)$ is neither constant over time nor equal for all targets, and setting the corresponding filter parameter $\hat{\gamma}(\cdot)$ is difficult. In some cases, the function $\gamma(\cdot)$ can be modeled using basic properties of the sensor that is used, see e.g. [12] for a practical example involving laser range sensors. Alternatively, the Poisson rates can be estimated from the sequence of measurement sets. A Bayesian framework for estimation of multiple Poisson rates for targets of different size and at different distance from the sensor is presented in [13]. The conjugate prior for the Poisson rate is the Gamma distribution [14], and exponential forgetting is used for prediction. An example where the measurement rates of three targets are estimated is given in Figure 3.

It should be noted that the actual sensor measurements does not have to be Poisson distributed in number, this is just a model. Indeed, the extended target PHD filter has been applied successfully to laser range data, which is not Poisson distributed in number, see [9], [10], [12]. What is important is that there is a model by which an estimate of γ can be obtained, using information from the previous sets of measurements, and possibly also a model of the sensor. In Figure 1, this corresponds to predicting the number of measurements that the car, bicyclist and pedestrian will cause, respectively.

C. Probability of detection

Similarly to γ , in [9], [10] the probability of detection $p_D(\mathbf{x})$ is approximated as a function of the target estimates, $p_D(\mathbf{x}) \approx p_D(\hat{\mathbf{x}})$. In some scenarios it is sufficient to assume that the probability of detection is constant in the surveillance volume. For the laser range sensor this assumption does not hold, because any target located behind another target is occluded from sensor view, and will not give any sensor detections. In this case, the probability of detection can be modeled

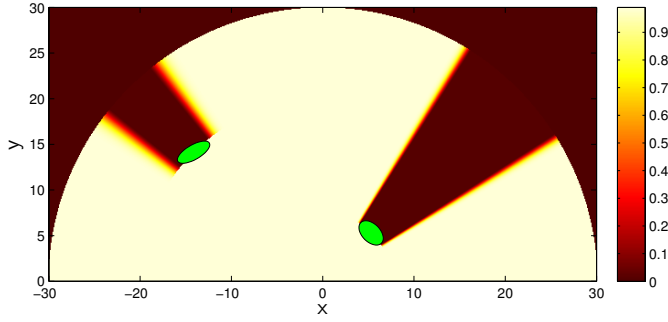


Fig. 4. Variable probability of detection. Behind the two extended target estimates (green ellipses) the probability of detection is lower. Plot created using the method from [10].

as a non-homogeneous function of the target estimates [9], [10], see Figure 4 for an example using the method presented in [10]. With a non-constant p_D the tracking filter can handle target occlusion, i.e. the filter can track targets as they move through areas in which they do not give any detections [9], [10].

In a general scenario, the probability of detection would also depend on factors such as the reflectivity of the object, its cross section, etc. In case such quantities are included into the state vector, and those states are observable, they can be included in the probability of detection calculations. Further information on probability of detection is given in, e.g., [1]–[3].

D. Different extended target representations

There are different ways to model the measurement distribution of multiple extended targets under association uncertainty and clutter. In this section two alternatives are highlighted, the commonly used Gaussian model, and the Gaussian inverse Wishart model first applied to target tracking by Koch [15], see also [16]. Some measurement models that can be used with each extended target model are also highlighted.

1) *Gaussian Mixture PHD*: In [8], [9], [12], the extended target PHD intensity is approximated as a Gaussian mixture,

$$D_{k|k}(\mathbf{x}|\mathbf{Z}) = \sum_{i=1}^{J_{k|k}} w_{k|k}^{(i)} \mathcal{N}(\mathbf{x}_k; m_{k|k}^{(i)}, P_{k|k}^{(i)}). \quad (4)$$

Here the state vector \mathbf{x}_k contains all parameters, from position and velocity to the parameters governing the size and shape of the extended targets. Using Gaussian mixtures to model the target distribution is a common choice in target tracking literature.

A possible measurement model is

$$p(\mathbf{z}_k|\mathbf{x}_k) = \mathcal{N}(\mathbf{z}_k; h_k(\mathbf{x}_k), R_k). \quad (5)$$

For the setup in Figure 1, the humans can be represented by state vectors that contain the position and velocity,

$$\mathbf{x} = [x \quad y \quad v_x \quad v_y]^T, \quad (6)$$

and the measurement model can be modelled as a linear function $h(\mathbf{x}) = H\mathbf{x}$, where $H = [\mathbf{I}_d, \mathbf{0}_d]^T$ and $d = 2$

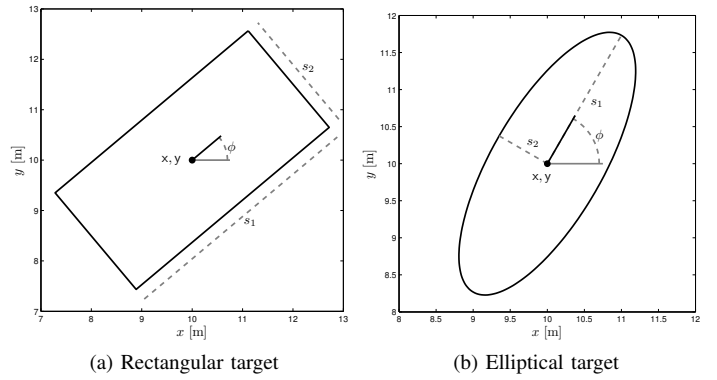


Fig. 5. Relationship between target states (7) and target shape. Plots from [12].

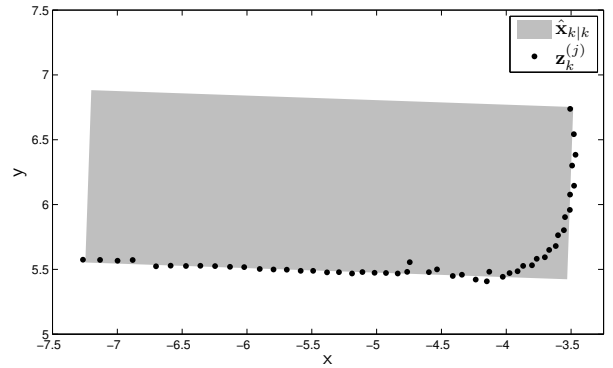


Fig. 6. Rectangular target, target state vector \mathbf{x} is given in (7). This type of extended target model is used in [12].

is the dimension of the measurements. This is performed successfully in [9].

The car in Figure 1 can be represented by a rectangle with state vector

$$\mathbf{x} = [x \quad y \quad v_x \quad v_y \quad \phi \quad s_1 \quad s_2]^T, \quad (7)$$

see Figure 5a for an explanation of the individual states. Figure 6 shows this extended target model applied to the L-shaped cluster of measurements in Figure 1. As an alternative to tracking the pedestrian's center of mass, a pedestrian can be represented as an ellipse, with state vector (7), see Figure 5b for an explanation of the individual states. Tracking of elliptical and rectangular extended targets, parametrised as in (7) and using laser range data, is performed in [12].

Non-linear measurement models have also been used to estimate polynomial structures in radar data [17], and to estimate general shapes in laser range data [18]. The bin-occupancy filter [19], which aims at estimating the probability of a target being in a given point, and whose continuous form is the same as the PHD filter, has been used to estimate an intensity based map of large and general shaped extended targets in [20].

2) *Gaussian inverse Wishart PHD*: In [10], the extended target PHD intensity is modeled as a Gaussian inverse Wishart

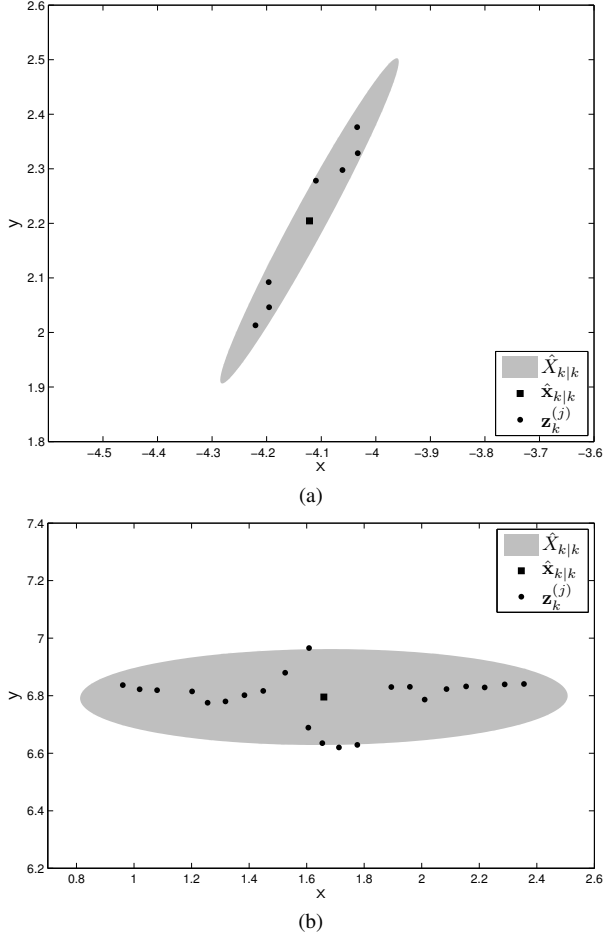


Fig. 7. Extended targets modelled with random matrices, showing data from a pedestrian (top) and a bicycle (bottom). The kinematical state is \mathbf{x}_k , the extension state is X_k . This type of extended target model is used in [10].

(GIW) mixture,

$$D_{k|k}(\xi|\mathbf{Z}) = \sum_{i=1}^{J_{k|k}} w_{k|k}^{(i)} \mathcal{N}(\mathbf{x}_k; m_{k|k}^{(i)}, P_{k|k}^{(i)}) \times \mathcal{IW}(X_k; v_{k|k}^{(i)}, V_{k|k}^{(i)}). \quad (8)$$

Here the extended target state ξ_k decomposes into a kinematical state \mathbf{x}_k , containing position, velocity and acceleration, and an extension state X_k , governing the shape and size. Thus, ξ_k in (8) is analogous to \mathbf{x}_k in (4). The extension state X_k is a positive definite symmetric random matrix, hence using Gaussian inverse Wishart (GIW) distributions to model the extended targets is also called the random matrix framework. In this framework, the extended targets are shaped as ellipses.

In the random matrix framework, a possible measurement model is

$$p(\mathbf{z}_k|\xi_k) = \mathcal{N}(\mathbf{z}_k; h_k(\mathbf{x}_k), X_k), \quad (9)$$

i.e. the extension state X_k is the measurement covariance. The corresponding likelihood function is presented in [10]. For the kinematical state \mathbf{x}_k the measurement update is similar

to the non-linear Gaussian model, for the extension state see [10]. Figure 7 shows this model applied to the two clusters of measurements in Figure 1 that correspond to the pedestrian and bicyclist.

III. THE EXTENDED TARGET CPHD FILTER

The approximation of the multi target distribution with its first order moment, i.e. the PHD, and the Poisson assumption used to produce closed form expressions for the PHD filter update, represent a major loss of information.

In [21] it is shown that PHD filter's cardinality estimate decreases too much, compared to the optimal update, when there is no detection and the value of P_D used by the filter is high. In [22], it is shown that the opposite case also is problematic, i.e. when the P_D (used by the PHD filter) is low and there are measurements, the expected number of targets obtained by the PHD filter increases too much, compared to the optimal update.

The phenomenon can be explained with a simple example. Assuming no false alarms and a single target with existence probability P_E , then the expected number of targets should be exactly unity when there is a detection. However, with the PHD filter this number turns out to become $1 + P_E(1 - p_D)$, whose bias increases as p_D decreases.

For extended targets cardinality bias is also a problem. It can be observed e.g. when a variable probability of detection, as described above, is used and a target enters or exits an occluded area. When the target is on the edge of the occluded area, the probability of detection, as modelled in [9], [10], is neither close to one or zero. If there are measurements originating from the target, the subsequent measurement update will cause a bias in the cardinality estimate.

To solve this type of problems, Mahler developed the CPHD filter, which, in addition to the PHD, propagates the cardinality distribution in time. An extension of this work to extended targets was presented in [22].

An example, where $p_D = 0.7$, is used to compare the extended target CPHD and PHD filters, see Figure 8 and 9, respectively, is presented in [22]. In this experiment two humans are present, entering the surveillance area around time step $k = 20$ and $k = 40$, respectively. The second person walks behind the first person and is therefore occluded around time steps $k = 75 - 80$. The performance of the CPHD does not change during this time, while the cardinality estimate of the PHD filter is biased, especially as the target enters and exits the occluded area. From the figures it is also obvious that the PHD filter has a significantly biased sum of weights when there is no target occlusion.

IV. CONCLUDING REMARKS

This paper presented a brief summary of the following research undertaken at the division of Automatic Control at Linköping University:

- 1) Two implementations of the extended target PHD filter [6], one Gaussian mixture implementation [8], [9], and one Gaussian inverse Wishart implementation [10].

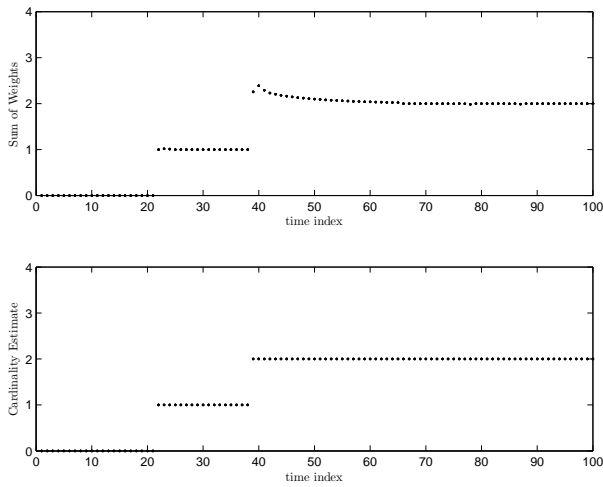


Fig. 8. The sum of weights (upper figure) and the cardinality estimates (lower figure) of the ETT-CPHD filter when nominal probability of detection is $P_D^0 = 0.7$. Figure from [22].

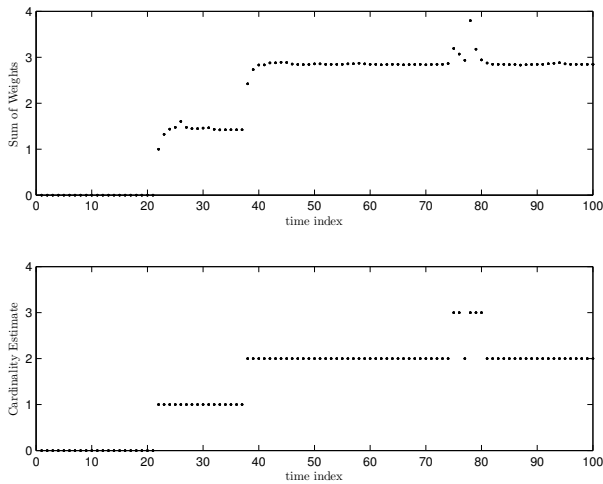


Fig. 9. The sum of weights (upper figure) and the cardinality estimates (lower figure) of the ETT-PHD filter when nominal probability of detection is $P_D^0 = 0.7$. Figure from [22].

- 2) Approaches to estimating the size and shape of extended targets, see [12], [18].
- 3) A Cardinalized PHD filter for multiple extended targets, see [22].

The research summarized in this paper has focused on tracking of moving targets. The simultaneous localisation and mapping (SLAM) problem has similarities to target tracking. An interesting and challenging direction for future work would be to consider also stationary targets, called landmarks, and to design an extended object SLAM algorithm.

ACKNOWLEDGMENT

The authors would like to thank the Linnaeus research environment CADICS and the frame project grant Extended Target Tracking (621-2010-4301), both funded by the Swedish

Research Council, as well as the project Collaborative Unmanned Aircraft Systems (CUAS), funded by the Swedish Foundation for Strategic Research (SSF), for financial support.

REFERENCES

- [1] Y. Bar-Shalom and T. E. Fortmann, *Tracking and data association*, ser. Mathematics in Science and Engineering. San Diego, CA, USA: Academic Press Professional, Inc., 1987, vol. 179.
- [2] Y. Bar-Shalom, *Multitarget-multisensor tracking: applications and advances*, ser. Multitarget-multisensor Tracking: Applications and Advances. Artech House, 1992, vol. II.
- [3] Y. Bar-Shalom, P. K. Willett, and X. Tian, *Tracking and data fusion, a handbook of algorithms*. YBS, 2011.
- [4] R. Mahler, "Multitarget Bayes filtering via first-order multi target moments," *IEEE Transactions on Aerospace and Electronic Systems*, vol. 39, no. 4, pp. 1152–1178, Oct. 2003.
- [5] —, *Statistical Multisource-Multitarget Information Fusion*. Norwood, MA, USA: Artech House, 2007.
- [6] —, "PHD filters for nonstandard targets, I: Extended targets," in *Proceedings of the International Conference on Information Fusion*, Seattle, WA, USA, Jul. 2009, pp. 915–921.
- [7] K. Gilholm, S. Godsill, S. Maskell, and D. Salmond, "Poisson models for extended target and group tracking," in *Proceedings of Signal and Data Processing of Small Targets*, vol. 5913. San Diego, CA, USA: SPIE, Aug. 2005, pp. 230–241.
- [8] K. Granström, C. Lundquist, and U. Orguner, "A Gaussian mixture PHD filter for extended target tracking," in *Proceedings of the International Conference on Information Fusion*, Edinburgh, UK, Jul. 2010.
- [9] —, "Extended Target Tracking using a Gaussian Mixture PHD filter," *IEEE Transactions on Aerospace and Electronic Systems*, 2012.
- [10] K. Granström and U. Orguner, "A PHD filter for tracking multiple extended targets using random matrices," *IEEE Transactions on Signal Processing*.
- [11] G.-C. Rota, "The number of partitions of a set," *The American Mathematical Monthly*, vol. 71, no. 5, pp. 498–504, May 1964.
- [12] K. Granström, C. Lundquist, and U. Orguner, "Tracking Rectangular and Elliptical Extended Targets Using Laser Measurements," in *Proceedings of the International Conference on Information Fusion*, Chicago, IL, USA, Jul. 2011, pp. 592–599.
- [13] K. Granström and U. Orguner, "Estimation and Maintenance of Measurement Rates for Multiple Extended Target Tracking," *Submitted to International Conference on Information Fusion*, 2012.
- [14] A. Gelman, J. B. Carlin, H. S. Stern, and D. B. Rubin, *Bayesian Data Analysis*, ser. Texts in Statistical Science. Chapman & Hall/CRC, 2004.
- [15] J. W. Koch, "Bayesian approach to extended object and cluster tracking using random matrices," *IEEE Transactions on Aerospace and Electronic Systems*, vol. 44, no. 3, pp. 1042–1059, Jul. 2008.
- [16] M. Feldmann, D. Fränken, and J. W. Koch, "Tracking of extended objects and group targets using random matrices," *IEEE Transactions on Signal Processing*, vol. 59, no. 4, pp. 1409–1420, Apr. 2011.
- [17] C. Lundquist, U. Orguner, and F. Gustafsson, "Extended target tracking using polynomials with applications to road-map estimation," *IEEE Transactions on Signal Processing*, vol. 59, no. 1, pp. 15–26, Jan. 2011.
- [18] C. Lundquist, K. Granström, and U. Orguner, "Estimating the Shape of Targets with a PHD Filter," in *Proceedings of the International Conference on Information Fusion*, Chicago, IL, USA, Jul. 2011, pp. 49–56.
- [19] O. Erdinc, P. Willett, and Y. Bar-Shalom, "The bin-occupancy filter and its connection to the PHD filters," *IEEE Transactions on Signal Processing*, vol. 57, no. 11, pp. 4232–4246, Nov. 2009.
- [20] C. Lundquist, L. Hammarstrand, and F. Gustafsson, "Road intensity based mapping using radar measurements with a probability hypothesis density filter," *IEEE Transactions on Signal Processing*, vol. 59, no. 4, pp. 1397–1408, Apr. 2011.
- [21] O. Erdinc, P. Willett, and Y. Bar-Shalom, "Probability hypothesis density filter for multitarget multisensor tracking," in *Proceedings of the International Conference on Information Fusion*, Philadelphia, CA, USA, July 2005, pp. 146–153.
- [22] U. Orguner, C. Lundquist, and K. Granström, "Extended Target Tracking with a Cardinalized Probability Hypothesis Density Filter," in *Proceedings of the International Conference on Information Fusion*, Chicago, IL, USA, Jul. 2011, pp. 65–72.